

## Degeneracy in $\text{Ag}_2\text{Te}$

C. WOOD, V. HARRAP, AND W. M. KANE

Research Division, Philco Corporation, Philadelphia, Pennsylvania

(Received August 24, 1960; revised manuscript received November 8, 1960)

The Hall coefficient, resistivity, and Seebeck coefficient of  $n$ - and  $p$ -type specimens of  $\text{Ag}_2\text{Te}$  have been measured over the temperature range from 55 to 300°K. These results indicate that the compound is highly degenerate over the whole temperature range studied. Calculations were made of the effective masses, mobility ratios, and energy gap and gave order of magnitude values.

### INTRODUCTION

THE first extensive investigation of the physical properties of the low-temperature or  $\beta$ -phase of  $\text{Ag}_2\text{Te}$  was reported by Appel,<sup>1</sup> who obtained a value for the forbidden energy gap of  $\sim 0.7$  ev by means of optical transmission measurements on thin films. Further work on this compound<sup>2</sup> was prompted by an interest in its thermoelectric properties and by the apparent contradiction between this relatively large energy gap and the low values for the Seebeck coefficient in fairly pure material.

The results obtained<sup>2</sup> disagreed with Appel's and indicated that the energy gap is extremely small, such that the material is intrinsic at room temperature, accounting for the small Seebeck coefficient. However, the Hall effect and resistivity data obtained were sufficient only to permit a classical analysis, whereas this material appears to be degenerate, even in the intrinsic range.

In the present work, additional measurements of Hall effect, resistivity, and Seebeck coefficient have been made allowing the degeneracy condition to be dealt with more effectively.

### MEASUREMENTS

#### Hall Effect

The Hall effect was measured by the conventional dc method, reversing the magnetic and electric fields for each measurement. No dependence of Hall effect

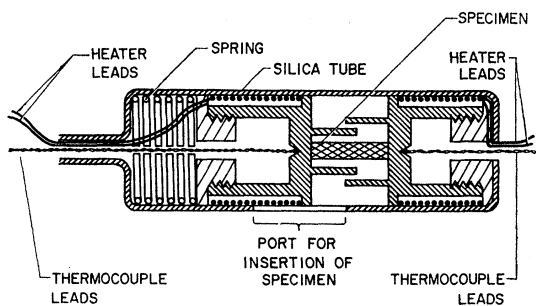


FIG. 1. Thermoelectric power apparatus.

<sup>1</sup> J. Appel, Z. Naturforsch. **10A**, 530 (1955).

<sup>2</sup> G. E. Gottlieb, W. M. Kane, J. F. Walsh, and C. Wood, J. Phys. Chem. Solids **15** (1960).

on magnetic field strength was observed up to fields of 6000 gauss.

#### Seebeck Coefficient

Measurements of the temperature dependence of the Seebeck coefficient were carried out in the apparatus shown in Fig. 1. Temperature differences between the specimen and contacts were minimized by enclosing the ends of the sample and the thermocouples by the copper contacts, i.e., approximating to black-body enclosures. A temperature difference of about 5°C was

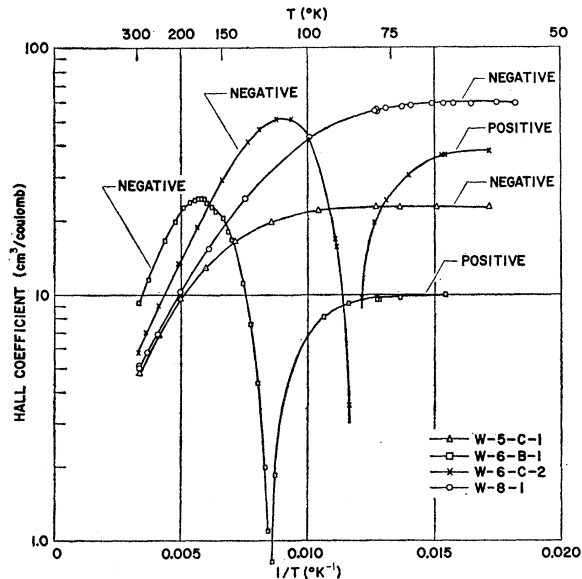


FIG. 2. Variation of Hall coefficient with reciprocal temperature for two  $n$ -type and two  $p$ -type specimens.

maintained between contacts by passing suitable electric currents through a heating coil, and was measured by means of calibrated chromel-constantan thermocouples. The resulting thermoelectric voltage across the specimen was measured by a Leeds and Northrup Type  $K$  potentiometer.

### RESULTS

The experimental values of Hall coefficient ( $R$ ), resistivity ( $\rho$ ), and Seebeck coefficient ( $Q$ ) are plotted as functions of temperature in Figs. 2, 3, and 4. These

measurements were performed on polycrystalline specimens produced by methods described elsewhere.<sup>3</sup> The specimens were etched with a 60%  $\text{NH}_4\text{OH}$ , 40%  $\text{H}_2\text{O}_2$  mixture. Unetched specimens gave slightly different results. The effect of etching appeared, in most cases, to change the position of the zero in the Hall-effect and Seebeck-coefficient curves to make the  $n$ -type specimens more  $p$ -type and the  $p$ -type specimens more  $n$ -type. X-ray examination of the etched and unetched specimens gave well-defined pictures in the etched case only, and henceforth only etched specimens were used for the measurements.

### DISCUSSION

The evaluation of the experimental data in  $\text{Ag}_2\text{Te}$  is complicated by the fact that the compound is highly degenerate at low temperatures (see below) and therefore the impurity concentrations and hence mobility ratios could not be accurately determined.

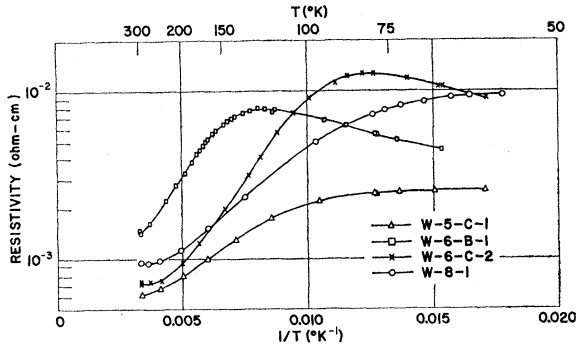


FIG. 3. Variation of resistivity with reciprocal temperature for two  $n$ -type and two  $p$ -type specimens.

Lack of knowledge of the position of the impurity levels in the energy bands prohibits the calculation of the degree of ionization of the impurities from the position of the Fermi-level.

### Degeneracy at Low Temperatures

Values for the Fermi level and effective mass were obtained from Hall data and the Seebeck coefficient ( $Q$ ) in the extrinsic range using the expressions

$$n, p = 4\pi \left( \frac{2m_{n,p}^* kT}{h^2} \right)^{3/2} F_{1/2}(\eta^*),$$

and

$$Q_{n,p} = \pm \left[ \frac{k[r+2] F_{r+1}(\eta^*)}{e[r+1] F_r(\eta^*)} - \eta^* \right],$$

where  $n$  = concentration of electrons in conduction band,  $p$  = concentration of holes in valence band,  $k$  = Boltzmann's constant,  $e$  = electronic charge,  $h$  = Planck's constant,  $m_{n,p}^*$  = effective mass of electrons or holes,

<sup>3</sup> P. F. Taylor and C. Wood, J. Appl. Phys. (to be published).

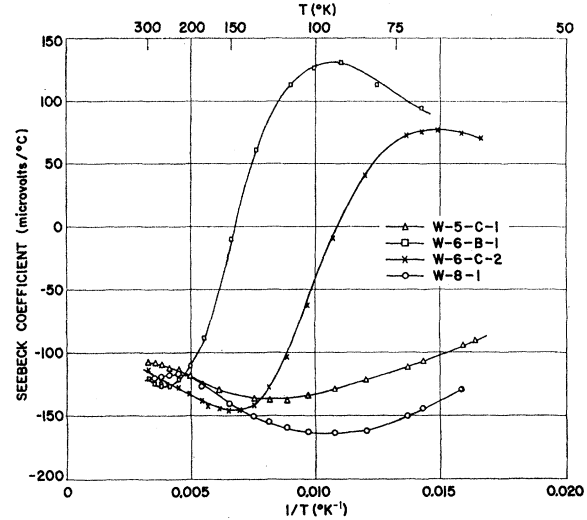


FIG. 4. Variation of Seebeck coefficient with reciprocal temperature for two  $n$ -type and two  $p$ -type specimens.

$T$  = absolute temperature,  $\eta^* = \eta/kT$  the reduced Fermi level measured from the relevant band edge,

$$F_r(\eta^*) = \int \frac{x^r dx}{1 + \exp(x - \eta^*)}, \quad \text{a Fermi-Dirac integral,}$$

and  $r$  = charge-carrier scattering constant.

In Table I the values of effective mass and Fermi level are listed assuming either scattering by lattice phonons ( $r=0$ ) or scattering by impurity ions ( $r=2$ ).

An unresolved part of our data is that the compound appears to be highly degenerate in the extrinsic range, and therefore the impurities are only partially ionized, however, the Hall constant becomes invariant with temperature at low temperatures. Measurements down to liquid helium temperatures on one specimen gave no variation of  $R$  with temperature. A possible explanation is that the impurity levels overlap the respective band edges so that the compound is really a semimetal.

### The Mobility Ratio

The value of  $b$  is usually estimated in  $p$ -type specimens from the values of the Hall constant ( $R$ ) as it

TABLE I. Values of effective mass and Fermi level, assuming either scattering by impurity ions ( $r=2$ ) or scattering by lattice phonons ( $r=0$ ).

Sample No.	Type	$T^\circ\text{K}$	$\eta^*$	$r=2$ $m_n^*$	$m_p^*$	$r=0$ $\eta^*$	$m_p^*$
W-8-1	$n$	71.5	4.7	0.027			
		63	5.7	0.026			
W-5-C-1	$n$	83.4	6.0	0.034			
		66.7	7.6	0.034			
W-6-B-1	$p$	77.0	7.0		0.057	2.1	0.16
		66.7	8.7		0.052	2.9	0.15
W-6-C-2	$p$	62.5	10.5		0.018	7.4	0.027
		58.9	11.0		0.018	7.8	0.027

TABLE II. Apparent values of  $b$  for four  $p$ -type specimens together with the intrinsic free-carrier concentration and temperature ( $T_{\max}$ ) at which  $R_{\max}$ , and therefore  $b$ , is measured.

Specimen No.	Free-hole conc. $\text{cm}^{-3}$	$T_{\max}$ $^{\circ}\text{K}$	$b$
<i>W 8</i> <sup>a</sup>	$8.8 \times 10^{16}$	103	5.8
<i>W 6C</i> <sup>a</sup>	$1.5 \times 10^{17}$	122	7.0
<i>W 6C2</i>	$1.63 \times 10^{17}$	110	7.3
<i>W 6B1</i>	$6.25 \times 10^{17}$	175	11.8

<sup>a</sup> Unetched specimens.

goes through a maximum ( $R_{\max}$ ) and the value in the extrinsic range ( $R_{\text{ex}}$ )

$$(b^2 - 1)/4b = -R_{\max}/R_{\text{ex}}.$$

Both  $R_{\max}$  and  $R_{\text{ex}}$  are dependent on the number of uncompensated impurity atoms,<sup>4</sup> and therefore on the position of the Fermi level at these two points. Apparent values of  $b$  for four  $p$ -type specimens together with the extrinsic free-carrier concentration and temperature ( $T_{\max}$ ) at which  $R_{\max}$ , and therefore  $b$ , is measured are given in Table II.

It is difficult to assess the relative importance of the effects of degeneracy and temperature on the value of  $b$ . If the effect of degeneracy is predominant then the lower values of  $b$  will be the more nearly correct values.

### Choice of Scattering Constant

Plots of  $R\sigma$  versus temperature in Fig. 5 for the  $n$ -type specimens show that  $r=0$  applies only at the higher temperature and not in the extrinsic range. For the  $p$ -type specimens five points on the Hall curves were chosen to determine values of hole mobility. It was assumed that  $b$  was constant with temperature and that  $N_a$  is given by the value of  $R_{\text{ex}}$ . When  $R=R_{\text{extrinsic}}$ ,

$$\mu_p = \sigma R_{\text{ex}}.$$

At  $R=0$ ,

$$\mu_p = \sigma(b-1)/eN_a b.$$

At  $R=R_{\max}$ ,

$$\mu_p = 2\sigma R_{\max}/(b-1).$$

When  $R=R_{\text{intrinsic}}$ ,

$$\mu_p = \sigma/e(nb+p).$$

$N$  and  $p$  were obtained from the general expression for the Hall coefficient

$$R = -\frac{n(b^2-1)-N_a}{e[n(b+1)+N_a]^2},$$

where  $N_a$  is the acceptor concentration. In all cases the scattering constant in the Hall expression was chosen to be unity, because of degeneracy.

The mobility curve for specimen *W 6B1* suggests that

<sup>4</sup> See for example N. B. Hannay, *Semiconductors* (Reinhold Publishing Corporation, New York, 1959), p. 395.

lattice scattering by acoustical modes is predominant over the whole temperature range, for which  $r=0$ . This agrees with results obtained on at least two other  $p$ -type specimens. The type of scattering in specimen *W 6C2* is less clear, and a valid choice of scattering factor was not held feasible.

### Thermal Activation Energy at Absolute Zero

The value of the energy gap at absolute zero was calculated from the slope of the plot of  $n\bar{p}/T^3$  versus  $1/T^{\circ}\text{K}$  for the  $p$ -type specimens (Fig. 6). The acceptor impurity concentration was assumed to be equal to the free-carrier concentration in the extrinsic range and the value of  $b$  was assumed to be independent of temperature. The discussion above shows that these assumptions may be invalid and therefore the final result may be in error.

Previous results<sup>2</sup> had indicated that the energy gap of  $\beta\text{-Ag}_2\text{Te}$  is extremely small, and therefore the  $n\bar{p}$  product is strictly given by

$$n\bar{p}/T^3 = (128\pi^2 k^2/h^5)(m_e m_p)^{3/2} F_{3/2}(\eta^*) F_{3/2}(-\eta^* - E^*).$$

The approximations for Fermi functions give an expression for the case of  $-\infty < \eta^* < +1.25$ , and where  $E^* > 2$ , of the form

$$\frac{n\bar{p}}{T^3} = 2.33 \times 10^{31} \frac{m_e m_p}{m^2} \exp\left(-\frac{1}{R} \frac{\partial E}{\partial T}\right) \times \exp\left(\frac{E_0}{RT}\right) [1 + 0.27 \exp \eta^*]^{-1}, \quad (1)$$

after the manner of Austin and McClymont.<sup>5</sup> Approxi-

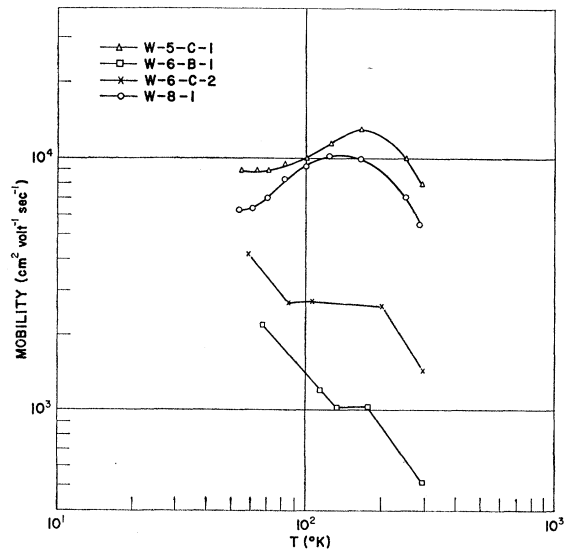


FIG. 5. Mobility variation with temperature for two  $n$ -type and two  $p$ -type samples.

mations<sup>6</sup> for  $\eta^* > 1$ , e.g.,  $F_{\frac{1}{2}}(\eta^*) + 0.667(\eta^{*2} + 1.645)^{\frac{1}{2}}$ , are not helpful in determining the energy gap, and the approximation for  $F_{\frac{1}{2}}(\eta^*)$  where  $\eta^* < 2$  (i.e., the classical case) cannot be used.

Calculations below, [see solution of Eq. (5)], show that in specimen *W 6B1* at 175°K, where  $R = R_{\text{max}}$ , the Fermi level is approximately  $2kT$  below the conduction band edge and  $E$  is also  $2kT$ . At 117°K, where  $R = 0$ , the Fermi level is  $4kT$  below the conduction band edge and  $E$  is  $3kT$ . Therefore, the conditions for Eq. (1) to apply are satisfied in this temperature range and the slope of the curve in Fig. 6 gives a value of  $\sim 0.05$  eV for the energy gap at absolute zero. The straight line is seen to actually extend from 150°K down to 100°K, below which inaccuracies in the small values of  $n$  prevented further calculation.

Similar calculations on specimen *W 6C2* showed that although the condition ( $E > 2kT$ ) for Eq. (1) to apply is not fully satisfied, a straight line of similar slope is obtained. The differing degrees of degeneracy of *W 6C2* and *W 6B1* may account for the fact that the two curves do not coincide.

### Thermal Activation Energy at Higher Temperatures

The Seebeck coefficient,  $Q$ , in the general case, when both holes and electrons are present is given by<sup>7</sup>

$$Q = (\sigma_n Q_n + \sigma_p Q_p) / (\sigma_n + \sigma_p), \quad (2)$$

where

$$Q_{n,p} = \pm \frac{k}{e} \left( \frac{r+2}{r+1} \frac{F_{r+1}(\eta^*)}{F_r(\eta^*)} - \eta^* \right), \quad (2a)$$

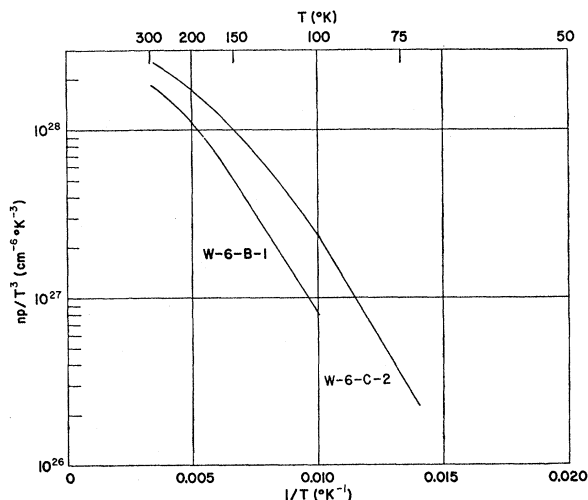


FIG. 6. Variation of  $np/T^3$  with reciprocal temperature for two *p*-type specimens.

<sup>5</sup> I. G. Austin and D. R. McClymont, *Physica* **20**, 1077 (1954).

<sup>6</sup> J. S. Blakemore, *Elec. Commun.* **29**, 131 (1952).

<sup>7</sup> V. A. Johnson, *Progress in Semiconductors* (John Wiley & Sons, Inc., New York, 1957), Vol. 1, p. 82.

TABLE III. Values of energy gap and effective mass for sample *W 6B1*, taking  $r=0$ .

<i>W 6B1</i>	
$E$	0.028 eV
$m_n/m_p$	0.71
$m_n/m_0$	0.12
$m_p/m_0$	0.17

$\sigma_n = ne\mu_n$  which is conductivity due to electrons,  $\sigma_p = pe\mu_p$  which is conductivity due to holes. This equation simplifies at  $R = R_{\text{max}}$ , where  $nb = p$ , to

$$Q = (Q_n + Q_p)/2, \quad (3)$$

and at  $R=0$ , where  $nb^2 = p$ , to

$$Q = (Q_n + bQ_p)/(1+b). \quad (4)$$

At  $R = R_{\text{max}}$ ,

$$b = \frac{p}{n} = \left( \frac{m_p}{m_n} \right)^{\frac{1}{2}} \frac{F_{\frac{1}{2}}(-\eta_m^* - E^*)}{F_{\frac{1}{2}}(\eta_m^*)},$$

where  $\eta_m^*$  is the reduced Fermi level at  $R_{\text{max}}$ . Similarly, at  $R=0$

$$b^2 = \frac{p}{n} = \left( \frac{m_p}{m_n} \right)^{\frac{1}{2}} \frac{F_{\frac{1}{2}}(\eta_0^* - E^*)}{F_{\frac{1}{2}}(\eta_0^*)},$$

where  $\eta_0^*$  is the reduced Fermi level at  $R_0$ . Hence

$$b = \frac{F_{\frac{1}{2}}(-\eta_0^* - E^*) F_{\frac{1}{2}}(\eta_m^*)}{F_{\frac{1}{2}}(\eta_0^*) F_{\frac{1}{2}}(-\eta_m^* - E^*)}. \quad (5)$$

If it is assumed that  $E^*$  and  $b$  are constant over the small temperature range between  $R=0$  and  $R=R_{\text{max}}$ , then it is possible to solve quite simply by graphical means for the unknowns  $\eta_0^*$ ,  $\eta_m^*$ , and  $E^*$  using Eqs. (3), (4), and (5). With this knowledge, values of effective mass can also be obtained. The values of energy gap and effective mass for sample *W 6B1*, taking  $r=0$ , are listed in Table III.

### Impurity Activation Energy

For nondegenerate conditions, and a constant Fermi level, Eq. (2a) becomes, for a one-carrier model,

$$Q = \pm \frac{k}{e} \left[ r+2 - \frac{E}{2kT} \right].$$

It is of interest that the Seebeck-coefficient curves when plotted as a function of reciprocal temperature ( $1/T^\circ\text{K}$ ) as in Fig. 5 give a value of  $E$  of about 0.02 eV in the extrinsic conductivity range, suggesting impurity levels in the middle of the forbidden gap. Too much importance must not be given to this result since it is known that the material is degenerate in this range.

## CONCLUSION

Thermal data, consisting of Hall, resistivity, and thermoelectric power indicate that in many respects  $\text{Ag}_2\text{Te}$  behaves as a conventional semiconductor with a very small forbidden energy gap. Calculations based on experimental data indicate variations of such parameters as mobility ratio, effective masses, and transport mechanism which are presumably dependent on composition and structure. The values calculated for these parameters are only indicative of the order of magnitude. Completely reliable figures could be

obtained only with considerably more experimental data.

The difference between the gap obtained from optical transmission data<sup>1</sup> and that obtained from thermal data could be due to a complex band structure, although discrepancies of this magnitude are not usually encountered in semiconductors.

## ACKNOWLEDGMENTS

We wish to thank G. E. Gottlieb for the production of the specimens and C. Hill for his helpful cooperation in performing the x-ray measurements.

## Effect of Static Strains on Diffusion

L. A. GIRIFALCO AND H. H. GRIMES

*Lewis Research Center, National Aeronautics and Space Administration, Cleveland, Ohio*

(Received September 16, 1960; revised manuscript received November 7, 1960)

A theory is developed that gives the diffusion coefficient in strained systems as an exponential function of the strain. This theory starts with the statistical theory of the atomic jump frequency as developed by Vineyard. The parameter determining the effect of strain on diffusion is related to the changes in the interatomic forces with strain. Comparison of the theory with published experimental results for the effect of pressure on diffusion shows that the experiments agree with the form of the theoretical equation in all cases within experimental error.

## I. INTRODUCTION

SINCE the diffusion rate in a crystal depends on the atomic interaction energy, and since this energy depends on the interatomic distances, it is to be expected that the diffusion coefficient of a migrating species will be altered by a strain superimposed on the crystal. Experimental evidence shows that the change in the diffusion coefficients resulting from strains can be considerable. Uniaxial elastic strain can increase the self-diffusion coefficient by as much as a factor of two<sup>1</sup> and large hydrostatic pressures may decrease the self-diffusion coefficient by as much as an order of magnitude.<sup>2-5</sup>

The theory of the effect of pressure on diffusion has been examined on the basis of the dynamic theory of diffusion.<sup>6,7</sup> In this theory, the pressure effect is represented by a parameter that is a function of the normal mode vibrations of the atoms in the crystal, and the diffusion coefficient is an exponential function of the pressure.

The dynamic theory of diffusion was developed as an alternative to the absolute rate theory of diffusion, since it was believed that the absolute rate theory depended on the postulate that the jumping atom spends a long time at the top of the potential barrier. However, it can be shown that the theory of the jump frequency can be developed without reference to such a postulate<sup>8</sup> by considering the motion of a representative point in phase space. The jump frequency then depends on the rate at which phase points move over the potential maximum in configuration space, and not on the length of time the phase points spend at the maximum. In view of this situation, it is of interest to investigate the effect of strain on diffusion in terms of the statistical rate theory.

The statistical rate theory of diffusion in strained crystals as developed in this paper shows that the diffusion coefficient is an exponential function of strain, and that the strain effect can be represented by a parameter that is a function of the interatomic forces. The rate theory, therefore, has an advantage over the dynamic theory in two respects: First, the effect of strain on diffusion in different materials can be correlated with the interatomic potential energy, and second, the interatomic forces provide a basis on which to calculate the magnitude of the strain effect for different diffusion mechanisms. Accordingly, the possibility pre-

<sup>1</sup> T. Liu and H. G. Drickamer, *J. Chem. Phys.* **22**, 312 (1954).

<sup>2</sup> Norman H. Nachtrieb, Wright Air Development Center Technical Report No. 55-68 (unpublished).

<sup>3</sup> J. Petit and N. H. Nachtrieb, *J. Chem. Phys.* **24**, 1027 (1956).

<sup>4</sup> W. Jost and G. Nehlep, *Z. physik. Chem.* **34**, 348 (1936).

<sup>5</sup> Norman H. Nachtrieb, Henry A. Resing, and Stuart A. Rice, *J. Chem. Phys.* **31**, 135 (1959).

<sup>6</sup> Stuart A. Rice, *Phys. Rev.* **112**, 804 (1958).

<sup>7</sup> Stuart A. Rice and Norman H. Nachtrieb, *J. Chem. Phys.* **31**, 139 (1959).

<sup>8</sup> George H. Vineyard, *J. Phys. Chem. Solids* **3**, 121 (1957).